ACS Catalysis

Letter

pubs.acs.org/acscatalysis

A Titanium−Organic Framework: Engineering of the Band-Gap Energy for Photocatalytic Property Enhancement

Ha L. Nguyen,*[,†,‡] Thanh T. Vu,[‡] Dinh Le,[‡] Tan L. H. Doan,[‡,§] Viet Q. Nguyen,[#] and Nam T. S. Phan*[,†]

[†]Faculty of Chemical Engineering, University of Technology, Vietnam National University−Ho Chi Minh City (VNU−HCM), Ho Chi Minh City 721337, Vietnam

[‡]Center for Innovative Materials and Architectures (INOMAR), Vietnam National University−Ho Chi Minh City (VNU−HCM), Ho Chi Minh City 721337, Vietnam

[§]Faculty of Chemistry, University of Science, Vietnam National University−Ho Chi Minh City (VNU−HCM), Ho Chi Minh City 721337, Vietnam

[#]National Key Lab for Polymer and Composite, University of Technology, Vietnam National University−Ho Chi Minh City (VNU−HCM), Ho Chi Minh City 721337, Vietnam

Supporting Information

ABSTRACT: A visible-light-responsive metal−organic framework based on titanium hexameric cluster and high conjugation system of organic linker building block termed MOF-902 was synthesized and fully characterized. The photocatalytic properties of MOF-902 were investigated in the polymerization reaction with various monomers such as methyl methacrylate (MMA), benzyl methacrylate (BMA), and styrene (St), respectively. Gel permeation chromatography (GPC) analysis results demonstrated the high performance of MOF-902 as a catalyst, affording polymer products with high molecular weight (M_n) and low polydispersity index (PDI). The photocatalytic efficiency of MOF-902 in the polymerization transformation obviously exceeds other catalysts such as MOF-901, UiO-66, UiO-66-NH_2, MIL-125(Ti), MIL-125-NH_2(Ti), and commercial P25-TiO_2.

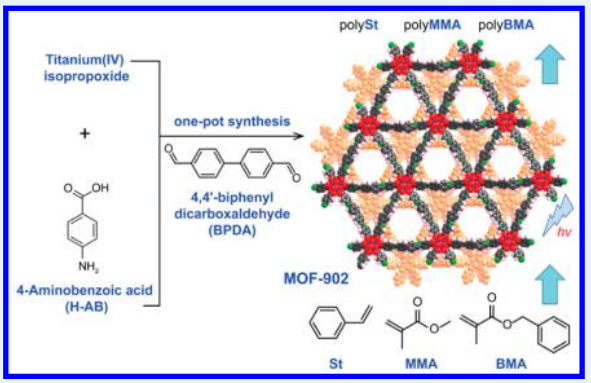

KEYWORDS: *titanium−organic framework, in situ cluster generation, photocatalysis, polymerization, band gap engineering*

Metal−organic frameworks (MOFs) have emerged as an advanced class of crystalline materials generated by the combination of organic linkers and metal clusters, termed "secondary building units".[1] MOFs have attracted significant attention over the past decade, because of their prominent properties including thermally and chemically stable features, high porosity, and tailorable structure, offering potential applications in many fields, such as gas capture and storage, separation, energy transformation, and catalysis.[2]

Photoactive materials based on MOFs have recently gained considerable interest from both industry and academia, because of the high optical responsibility needed to make progress with regard to pollutant degradation,[3] water splitting,[4] CO_2 reduction,[5] and photocatalysis application.[6] Among several popular photocatalytic structures,[7] MOFs containing the oxophilic titanium cluster (Ti−oxo cluster), for example, MIL-125, and MIL-125-NH_2 are well-established photocatalytic materials, which are useful in photosynthesis, water treatment, and photocatalysis applications, because of their low toxicity and high performance in redox reactions and photoactivity.[8] However, reports on utilization of Ti-MOFs as heterogeneous photocatalysts have been limited in the literature, because of the problems of dynamic dissociation Ti−O bonding during the synthesis process leading to obtain few crystalline Ti-MOFs.[9]

In previous research, we reported the novel approach to synthesize visible-light-responsive titanium−organic framework 901 (MOF-901),[9a] which is constructed through imine condensation reaction linking the *in situ* $Ti_6O_6(OMe)_6(AB)_6$ (AB = 4-aminobenzoate) clusters with 1,4-benzenedialdehyde (BDA) constituents. In this communication, we would like to present a strategy to further engineering the optical absorption features for a water-stable and chemically stable Ti-MOF, named MOF-902, which is isoreticular structure to MOF-901, by exploiting the *in situ* cluster formation technique (Figure 1).

Especially, the longer linking unit containing two benzene rings was introduced into the MOF-902 framework to exploit the high conjugation backbone, which could contribute to resulting in the visible-light absorption in red-shifted region.[6a] The photoactivity of MOF-902 was demonstrated in the

Received: September 14, 2016
Revised: December 1, 2016
Published: December 6, 2016

DOI: 10.1021/acscatal.6b02642
ACS Catal. 2017, 7, 338−342

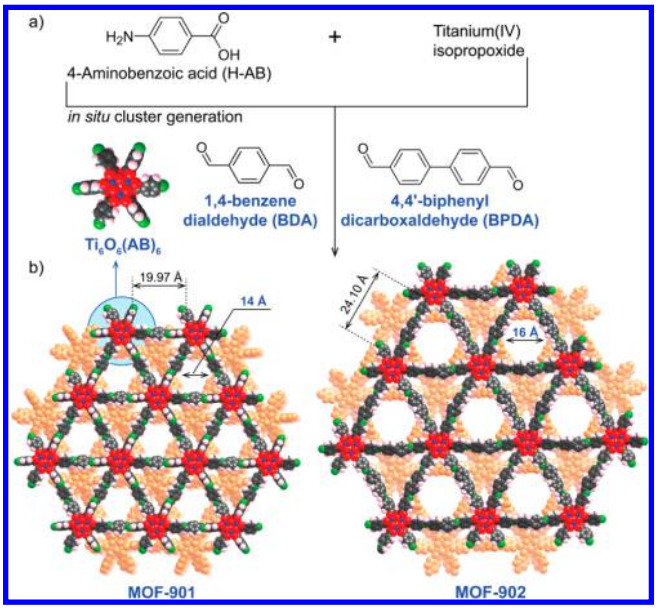

Figure 1. Synthetic procedure depicting the strategy to produce MOF-901, MOF-902 based on (a) the *in situ* Ti−oxo cluster generation and aldehyde functionalities and (b) the space filling model of crystal structure of MOF-901 and isoreticular MOF-902, which contains the longer aldehyde linking unit. Atom colors: Ti, blue; C, black; O, red; N, green; H, pink; and second layer, orange. Capping methoxide moieties have been removed for clarity.

photopolymerization reaction under visible light. Interestingly, MOF-902 outperforms the photocatalytic property of the commercial catalyst P25-TiO_2, MOF-901, as well as other photoactive MOFs such as UiO-66, UiO-66-NH_2, MIL-125(Ti), and MIL-125-NH_2(Ti).

MOF-902 was solvothermally synthesized with slight modifications to MOF-901 in a previous report.[9a] Specifically, 4,4′-biphenyldicarboxaldehyde (BPDA) was dispersed in methanol before adding to the methanolic solution containing the mixture of 4-aminobenzoic acid (H-AB) and titanium(IV)-isopropoxide. The mixture was introduced to a Teflon vessel and transferred to a stainless steel autoclave, which was then heated at 140 °C for 3 days, yielding a yellow microcrystalline solid. The crystal structure and photocatalytic properties of MOF-902 were subsequently characterized after solvent exchange and activation steps (see the Supporting Information (SI), Section S2).

The presence of imine linkage was initially supported by Fourier transform infrared (FT-IR) spectroscopy, which clearly displayed the characteristic of imine-derived C═N ($\nu_{C=N}$ = 1625.8 cm^{-1}) and C−C═N−C ($\nu_{C-C=N-C}$ = 1199.4 cm^{-1}) stretching vibration frequencies (SI, Section S3). The methoxide caps were determined by digested ^1H NMR spectroscopy which corresponds to the singlet resonance at 3.5 ppm (SI, Section S4). Note that MOF-902 is an isoreticular structure of MOF-901 and could not be obtained as a single crystal. The structural elucidation for MOF-902 was carried out on an activated sample, which was applied to measure powder X-ray diffraction (PXRD) analysis (SI, Section S5). Specifically, a structural model was built by linking the hexameric 6-connected (6-c) $Ti_6O_6(OMe)_6(AB)_6$ SBUs with the linear 4,4′-biphenyldicarboxaldehyde (BPDA) linkers into a 6,2-c **hxl** topology (SI, Section S5). The modeling was first executed with two possibilities, including fully eclipsed version and staggered stacking mode of the layers. The staggered model was then adopted because of the stacking space of the layers, leading to the optimized void space of two-dimensional (2D) stacking sequence. The refined unit-cell parameters ($P6_3$, a = 31.4453(6) Å, c = 7.7346(5) Å) and satisfactory residual values (R_p = 2.68%, R_{wp} = 3.52%) were obtained after a full profile pattern refinement against the experimental PXRD pattern (SI, Section S5). The 2D structure of MOF-902 is constructed based on imine linking units, which are generated by imine condensation reaction from six terminal ligands chelating to a trigonal prismatic Ti_6O_6 inner core of six points of extension SBU. Every second layer of **hxl** eclipsed network in MOF-902 is translated to generate the Ti_6O_6 SBUs to the center of triangular windows of the first layer resulting in the staggered version, in which a ca. 16 Å diameter of the hexagonal window was found to be larger than in the case of MOF-901 (in ca. 14 Å, Figure 1). Thermogravimetric analysis (TGA) further supports the formulation of MOF-902 by the residual coincidence of TiO_2 residue between experimental and theory (SI, Section S6). In addition, the potential solvent accessible void, as calculated by PLATON,[10] is 40%, which is insignificantly higher than the value supported by N_2 isotherm measurements at low pressure and 77 K. Brunauer−Emmett−Teller (BET) and Langmuir surface areas of 400 and 600 m^2 g^{-1}, respectively, were achieved for the Ti-MOF (SI, Section S7).

The optical absorption property of MOF-902 was studied by UV-vis diffuse reflectance spectroscopy (UV-DRS) analysis (SI, Section S8). It was observed that MOF-902 clearly exhibits a broad range of optical absorption from 340 nm to 640 nm, in which the maximum absorption would be located at 390 nm, corresponding to the yellow color of activated sample. This visible-light absorption spectrum is dramatically red-shifted, in comparison with other photoactive MOFs (Table 1). Especially, the band-gap energy of MOF-902, which was calculated from a Tauc plot, was found to be ∼2.50 eV (Figure 2). The high conjugation system of linking unit present in the structural backbone of MOF-902 would result in the red-shifted visible light absorption. This observation was in good agreement with previous reports in the literature, in which the effects of high conjugation bridging units to optico-chemical property of MOF materials was investigated.[11] The longer organic building blocks in the structure of MOF-902 undoubtedly support a reduction in the band-gap energy, compared to MOF-901. Indeed, the main absorption bands of MOF-902 are located in the visible-light region (340−640 nm), which could not only be attributed to ligand-to-metal charge transfer (LMCT)[6a,11a] but also could be demonstrated by the lone-pair electron of nitrogen for the interaction with the π^*-orbitals from the imine linkage. This would donate electron density to the antibonding orbitals, which leads to a higher HOMO level that improve the optical absorption property.[11] This optical band gap energy is also slightly lower than that of MIL-125-NH_2(Ti), MOF-901, and UiO-66-NH_2, but higher than the case of PCN-22 and NTU-9 (see Table 1).[12−15]

The photoactivity of MOF-902 was demonstrated by performing the polymerization reaction of methyl methacrylate (MMA) under visible light in the presence of ethyl α-bromophenylacetate as a co-initiator (SI, Section S9). In a previous study, we reported that MOF-901 could catalyze the polymerization reaction of MMA, resulting in high-molecular-weight polyMMA (26 850 g mol^{-1}) and a reasonable polydispersity index (PDI) (1.6). Interestingly, we found that the PDI of polyMMA could be decreased dramatically when

DOI: 10.1021/acscatal.6b02642
ACS Catal. 2017, 7, 338−342

Table 1. Summary for Photoabsorption Properties of MOF-902 and Other Related MOFs

MOF	SBU	band gap (eV)	linker	ref
UiO-66	$Zr_6O_4(OH)_4(CO_2)_{12}$	4.07	BDC[a]	12
UiO-67	$Zr_6O_4(OH)_4(CO_2)_{12}$	3.68	BPDC[b]	12
MIL-125(Ti)	$Ti_8O_8(OH)_4(CO_2)_{12}$	3.60	BDC	8
VNU-2	$Hf_6O_4(OH)_4(CO_2)_{12}$	3.36	CPEB[c]	6a
P25-TiO_2[d]	TiO_2	3.20		13
UiO-66-NO_2	$Zr_6O_4(OH)_4(CO_2)_{12}$	3.10	BDC-NO_2	14
VNU-1	$Zr_6O_4(OH)_4(CO_2)_{12}$	2.88	CPEB	6a
UiO-66-NH_2	$Zr_6O_4(OH)_4(CO_2)_{12}$	2.75	BDC-NH_2	15
MOF-901	$Ti_6O_6(OMe)_6(CO_2)_6$	2.65	PMAB[e]	9a
MIL-125-NH_2(Ti)	$Ti_8O_8(OH)_4(CO_2)_6$	2.60	BDC-NH_2	8
MOF-902	$Ti_6O_6(OMe)_6(CO_2)_6$	2.50	BMAB[f]	this work
PCN-22	$Ti_7O_6(OH)_4(CO_2)_{12}$	1.93	TCPP[g]	9b
NTU-9	$Ti(OH)_2(CO_2)_2$	1.72	DOBDC[h]	9e

[a]BDC = 1,4-benzenedicarboxylate. [b]BPDC = Biphenyl-4,4′-dicarboxylate. [c]CPEB = 1,4-bis(2-[4-carboxyphenyl]ethynyl)benzene. [d]Commercial photocatalyst P25-TiO_2, which cannot be classified as a MOF, is presented here to clarify the band gap energy comparison to other MOFs used as heterogeneous photocatalysts. [e]PMAB = 1,4-phenylenebis(methanylylidene)bis(azanylylidene)dibenzoate; this linker was generated through imine condensation reaction during the one-pot synthesis of MOF-901. [f]BMAB = biphenyl-4,4′-diylbis-(methanylylidene)bis(azanylylidene)dibenzoate; this linker was generated through imine condensation reaction during the one-pot synthesis of MOF-902. [g]TCPP = tetrakis(4-carboxyphenyl)porphyrin. [h]DOBDC = 2,5-dihydroxybenzenedicarboxylate.

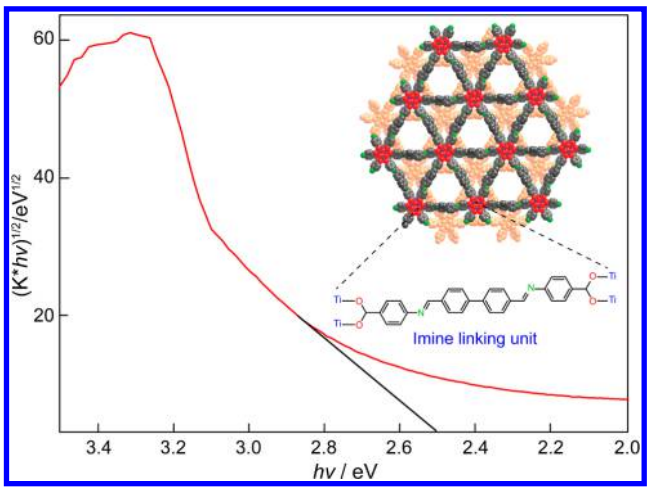

Figure 2. Optical band-gap energy of activated MOF-902. Inset: The crystal structure of MOF-902 was presented to clarify the linking unit that could partly contribute to reducing the band-gap energy of MOF-902, as well as its high photocatalysis property, compared to MOF-901.

MOF-902 was used as the catalyst for the reaction under identical conditions. Indeed, the transformation produced polyMMA with high molecular weight (31 465 g mol^{-1}), high yield (84%), and uniform distribution, as indicated by the very low PDI (1.11). The high conjugation system of imine linking units of MOF-902 containing more electron donor than MOF-901 contributed to stabilize the free radicals during the reaction process, to afford dormant polymer chains with a bromide end group. It was previously reported that stable radicals have a tendency to locate at the unpaired electron region with good steric protection or near at the conjugated systems exhibiting resonance stabilization.[16] This phenomenon caused fast visible-light initiation and rapid recapping of the radical chain end with bromide, leading to a uniform growth of all the polymer chains.[17] In addition, polymer chain termination could also be minimized as a result of the low stationary concentration of propagating radicals, thus contributing to generate high yield and low PDI.[17] These observations would confirm that MOF-902 clearly outperforms the commercial catalyst P25-TiO_2, MOF-901, as well as other MOFs possessing similar band-gap energies (see Table 2).

Table 2. Polymerization Reaction of Methylmethacrylate under Visible Light in the Presence of Diverse Photocatalysts[a]

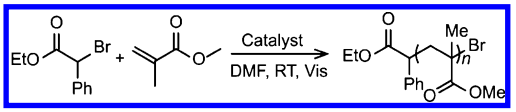

entry	catalyst (mol %)	yield (%)	M_n (g mol^{-1})	M_w/M_n
MOF-902[b,c]	0.034	84	31 465	1.11
MOF-901[b,d]	0.034	87	26 850	1.60
MOF-902	0	nd	na	na
MOF-901	0	nd	na	na
P25-TiO_2[b]	0.034	52	17 000	1.62
UiO-66[b]	0.034	nd	na	na
UiO-66-NH_2[b]	0.034	13	18 500	1.61
VNU-1[b]	0.034	nd	n.a.	n.a.
MIL-125[b]	0.034	nd	n.a.	n.a.
MIL-125-NH_2[b]	0.034	nd	n.a.	n.a.

[a]Reaction performed without catalyst. nd = not detected (or trace which cannot be isolated); na = not applicable; M_n = number-average molar mass; M_w = mass average molar mass. [b]Reaction conditions: MMA (2.0 M in *N*,*N*-dimethylformamide), catalyst (0.034 mol %), and ethyl α-bromophenylacetate (0.61 mol %) at room temperature with visible light from a compact fluorescent light bulb (4U, 55 W) for 18 h. [c]MOF-902 with a median particle size of 30 μm, while 50% yield, M_n of 21 470 g mol^{-1}, and PDI of 1.22 were observed for pristine MOF-902 with a median particle size of 45 μm. [d]The GPC result was used from a previous publication (ref 9a); polyMMA was also reproduced to confirm the previous results.

In order to further investigate the visible light photoresponsive properties of MOF-902, which is hypothesized to affect the photocatalytic performance, other monomers such as benzyl methacrylate (BMA) and styrene (St), respectively, were utilized for the polymerization reaction. In addition, the effect of organic solvents was also studied by conducting the transformation under an identical synthetic procedure (SI, Section S9). It was observed that MOF-902 could be used as an efficient photocatalyst to promote the polymerization reaction of MMA, BMA in several organic solvents such as *N*,*N*-dimethylformamide (DMF), tetrahydrofuran (THF), or 1,4-dioxane. Interestingly, MOF-902 generated polyMMA and polyBMA with high molecular weight (22 330 and 32 050 g mol^{-1}, respectively) and very low polydispersity index (1.19 and 1.11, respectively) in 1,4-dioxane. Similarly, for the polymerization reaction carried out in DMF or THF, MOF-902 also exhibited significantly better performance than MOF-901. MOF-902 was also more profitable than MOF-901 in the formation of polySt in THF with a molecular weight of 6660 g mol^{-1} and a reasonable PDI of 1.65 (see Table 3).

DOI: 10.1021/acscatal.6b02642
ACS Catal. 2017, 7, 338−342

Table 3. Studies of MOF-902 Catalysis Property with Various Monomers, in Comparison to MOF-901[a]

solvent	catalyst	yield (%)	M_n (g mol^{-1})	M_w/M_n
		MMA Monomer[b]		
DMF	MOF-901[c]	87	26 850	1.60
DMF	MOF-902[d]	84	31 465	1.11
THF	MOF-901	nd	na	na
THF	MOF-902	45	21 700	1.24
dioxane	MOF-901	nd	na	na
dioxane	MOF-902	28	22 330	1.19
		BMA Monomer[b]		
DMF	MOF-901	nd	na	na
DMF	MOF-902	80	27 800	1.16
THF	MOF-901	39	29 778	1.14
THF	MOF-902	95	23 434	1.11
dioxane	MOF-901	nd	na	na
dioxane	MOF-902	71	32 050	1.11
		St Monomer[b]		
DMF	MOF-901	nd	na	na
DMF	MOF-902	nd	na	na
THF	MOF-901	nd	na	na
THF	MOF-902	13	6660	1.65
dioxane	MOF-901	nd	na	na
dioxane	MOF-902	nd	na	na

[a]nd = not detected (or trace which cannot be isolated); na = not applicable; M_n = number-average molar mass; M_w = mass average molar mass. [b]Reaction conditions: monomer (2.0 M in organic solvent), catalyst (0.034 mol %), and ethyl α-bromophenylacetate (0.61 mol %) at room temperature with visible light from a compact fluorescent light bulb (4U, 55 W) for 18 h. [c]The GPC result was used from previous publication (ref 9a); polyMMA was also reproduced to confirm the previous results. [d]MOF-902 with a median particle size of 30 μm.

The recyclability of MOF-902 as a heterogeneous photocatalyst was validated through recycling study (see Table 4, as well as SI, Section S9). Especially, MOF-902 was first isolated after 18 h of reaction time by centrifugation. Physisorbed reagents in the pores of MOF-902 was subsequently removed by washing the catalyst with dichloromethane several times. MOF-902 was then immersed in methanol for 5 h before regeneration under vacuum at 120 °C. Remarkably, the crystallinity as well as the heterogeneous photocatalytic nature of MOF-902 was retained, as proven by powder XRD patterns, and GPC analysis results. Indeed, experimental results displayed that the photoactivity of MOF-902 still remained without a significant loss of performance over at least five consecutive cycles. Note that MOF-901 was almost inactive for the first run under identical conditions, with polyBMA being detected only in trace amounts.

Table 4. Recycling Study of MOF-902 in Polymerization Reaction of BMA in 1,4-Dioxane under Visible Light

photorecycling number	yield (%)	M_n (g mol^{-1})	M_w/M_n
1st	71	32 050	1.11
2nd	70	31 700	1.12
3rd	72	32 000	1.11
4th	70	30 450	1.20
5th	68	30 025	1.16

In conclusion, we have reported the synthesis of MOF-902 constructed from a hexameric titanium $Ti_6O_6(OMe)_6(AB)_6$, which is formed via *in situ* generation and 4,4′-biphenyldicarboxaldehyde (BPDA). The crystal structure of MOF-902 was analyzed by powder X-ray diffraction (PXRD) and supported analyses. By incorporating the highly conjugated imine linking unit, MOF-902 absorbs the visible light in the red-shift region, leading to a low band-gap energy (ca. 2.50 eV). The visible-light-responsive activity of MOF-902 was confirmed by the enhancement in the photocatalytic properties. MOF-902 exhibited high performance in photocatalysis application of polymerization reaction with various monomers such as methyl methacrylate (MMA), benzyl methacrylate (BMA), and styrene (St), resulting in high molecular weight (M_n) and low polydispersity index (PDI) of polymer products. Containing a higher conjugation system of linking building units in the framework, MOF-902 exhibited significantly better performance as a heterogeneous photocatalyst than MOF-901 in polymerization reactions. The photocatalysis property of MOF-902 also outperforms the commercial catalyst P25-TiO_2, as well as other MOFs possessing similar band-gap energies.

■ ASSOCIATED CONTENT

Supporting Information

The Supporting Information is available free of charge on the ACS Publications website at DOI: 10.1021/acscatal.6b02642.

Synthesis and characterization details of MOF-902 including powder X-ray diffraction analysis data, computational modeling, supported analyses, and photocatalytic polymerization reaction measurements and data (PDF)

■ AUTHOR INFORMATION

Corresponding Authors

*E-mail: hanguyen@manar.edu.vn (H. L. Nguyen).
*E-mail: ptsnam@hcmut.edu.vn (N. T. S. Phan).

Funding

H.L.N. acknowledges funding for the catalytic application from Vietnam National University−Ho Chi Minh City (VNU−HCM) (No. INOMAR-CS2016-02). The synthesis of MOF-902 and imine linker was funded by VNU−HCM under grant number VNUB2017-50-01.

Notes

The authors declare no competing financial interest.

■ ACKNOWLEDGMENTS

H.L.N. acknowledges Prof. Dzung Hoang, and Dr. Thi T. Pham (INOMAR), Prof. Vinh Q. Lam (VNU−HCM), and Dr. Thu T. L. Nguyen (HCMUT) for the advanced discussion and supports during the manuscript revision.

■ REFERENCES

(1) (a) Li, M.; Li, D.; O'Keeffe, M.; Yaghi, O. M. *Chem. Rev.* **2014**, *114*, 1343−1370. (b) Alezi, D.; Peedikakkal, A. M. P.; Weseliński, Ł. J.; Guillerm, V.; Belmabkhout, Y.; Cairns, A. J.; Chen, Z.; Wojtas, Ł.; Eddaoudi, M. *J. Am. Chem. Soc.* **2015**, *137*, 5421−5430.

(2) (a) Furukawa, H.; Cordova, K. E.; O'Keeffe, M.; Yaghi, O. M. *Science* **2013**, *341*, 1230444. (b) Zhou, H.-C; Kitagawa, S. *Chem. Soc. Rev.* **2014**, *43*, 5415−5418. (c) Tu, T. N.; Phan, N. Q.; Vu, T. T.; Nguyen, H. L.; Cordova, K. E.; Furukawa, H. *J. Mater. Chem. A* **2016**, *4*, 3638−3641.

(3) (a) Hou, Y. L.; Sun, R. W.; Zhou, X. P.; Wang, J. H.; Li, D. *Chem. Commun.* **2014**, *50*, 2295−2297. (b) Laurier, K. G. M.; Vermoortele, F.; Ameloot, R.; De Vos, D. E.; Hofkens, J.; Roeffaers, M. B. J. *J. Am. Chem. Soc.* **2013**, *135*, 14488−14491.

DOI: 10.1021/acscatal.6b02642
ACS Catal. 2017, 7, 338−342

(4) (a) Du, P.; Eisenberg, R. *Energy Environ. Sci.* **2012**, *5*, 6012−6021. (b) Wang, J.-L.; Wang, C.; Lin, W. *ACS Catal.* **2012**, *2*, 2630−2640.
(5) (a) Fu, Y.; Sun, D.; Chen, Y.; Huang, R.; Ding, Z.; Fu, X.; Li, Z. *Angew. Chem., Int. Ed.* **2012**, *51*, 3364−3367. (b) Wang, S.; Yao, W.; Lin, J.; Ding, Z.; Wang, X. *Angew. Chem., Int. Ed.* **2014**, *53*, 1034−1038.
(6) (a) Doan, T. L. H.; Nguyen, H. L.; Pham, H. Q.; Pham-Tran, N.-N.; Le, T. N.; Cordova, K. E. *Chem. - Asian J.* **2015**, *10*, 2660−2268. (b) Nasalevich, M. A.; Goesten, M. G.; Savenije, T. J.; Kapteijn, F.; Gascon, J. *Chem. Commun.* **2013**, *49*, 10575−10577.
(7) (a) Wang, B.; Lv, X.-L.; Feng, D.; Xie, L.-H.; Zhang, J.; Li, M.; Xie, Y.; Li, J.-R.; Zhou, H.-C. *J. Am. Chem. Soc.* **2016**, *138*, 6204−6216. (b) Bai, Y.; Dou, Y.; Xie, L. H.; Rutledge, W.; Li, J. R.; Zhou, H.-C. *Chem. Soc. Rev.* **2016**, *45*, 2327−2367. (c) Smith, S. J. D.; Ladewig, B. P.; Hill, A. J.; Lau, C. H.; Hill, M. R. *Sci. Rep.* **2015**, *5*, 7823.
(8) (a) Hendon, C. H.; Tiana, D.; Fontecave, M.; Sanchez, C.; D'Arras, L.; Sassoye, C.; Rozes, L.; Mellot-Draznieks, C.; Walsh, A. *J. Am. Chem. Soc.* **2013**, *135*, 10942−10945. (b) Wang, H.; Yuan, X.; Wu, Y.; Zeng, G.; Dong, H.; Chen, X.; Leng, L.; Wu, Z.; Peng, L. *Appl. Catal., B* **2016**, *186*, 19−29.
(9) (a) Nguyen, H. L.; Gándara, F.; Furukawa, H.; Doan, T. L. H.; Cordova, K. E.; Yaghi, O. M. *J. Am. Chem. Soc.* **2016**, *138*, 4330−4333. (b) Yuan, S.; Liu, T.-F.; Feng, D.; Tian, J.; Wang, K.; Qin, J.; Zhang, Q.; Chen, Y.-P.; Bosch, M.; Zou, L.; Teat, S. J.; Dalgarno, S. J.; Zhou, H.-C. *Chem. Sci.* **2015**, *6*, 3926−3930. (c) Mason, J. A.; Darago, L. E.; Lukens, W. W.; Long, J. R. *Inorg. Chem.* **2015**, *54*, 10096−10104. (d) Dan-Hardi, M.; Serre, C.; Frot, T.; Rozes, L.; Maurin, G.; Sanchez, C.; Férey, G. *J. Am. Chem. Soc.* **2009**, *131*, 10857−10859. (e) Gao, J.; Miao, J.; Li, P.-Z.; Teng, W. Y.; Yang, L.; Zhao, Y.; Liu, B.; Zhang, Q. *Chem. Commun.* **2014**, *50*, 3786−3788.
(10) Spek, A. L. *J. Appl. Crystallogr.* **2003**, *36*, 7−13.
(11) (a) Pham, H. Q.; Mai, T.; Pham-Tran, N.-N.; Kawazoe, Y.; Mizuseki, H.; Nguyen-Manh, D. *J. Phys. Chem. C* **2014**, *118*, 4567−4577. (b) Lin, C.-K.; Zhao, D.; Gao, W.-Y.; Yang, Z.; Ye, J.; Xu, T.; Ge, Q.; Ma, S.; Liu, D.-J. *Inorg. Chem.* **2012**, *51*, 9039−9044. (c) Shen, L.; Liang, R.; Luo, M.; Jing, F.; Wu, L. *Phys. Chem. Chem. Phys.* **2015**, *17*, 117−121. (d) Long, J.; Wang, S.; Ding, Z.; Wang, S.; Zhou, Y.; Huang, L.; Wang, X. *Chem. Commun.* **2012**, *48*, 11656−11658.
(12) Chavan, S.; Vitillo, J. G.; Gianolio, D.; Zavorotynska, O.; Civalleri, B.; Jakobsen, S.; Nilsen, M. H.; Valenzano, L.; Lamberti, C.; Lillerud, K. P.; Bordiga, S. *Phys. Chem. Chem. Phys.* **2012**, *14*, 1614−1626.
(13) Dette, C.; Pérez-Osorio, M. A.; Kley, C. S.; Punke, P.; Patrick, C. E.; Jacobson, P.; Giustino, F.; Jung, S. J.; Kern, K. *Nano Lett.* **2014**, *14*, 6533−6538.
(14) Shen, L.; Liang, R.; Luo, M.; Jing, F.; Wu, L. *Phys. Chem. Chem. Phys.* **2015**, *17*, 117−121.
(15) Long, J.; Wang, S.; Ding, Z.; Wang, S.; Zhou, Y.; Huang, L.; Wang, X. *Chem. Commun.* **2012**, *48*, 11656−11658.
(16) (a) Faust, T. F.; D'Alessandro, D. M. *RSC Adv.* **2014**, *4*, 17498−17512. (b) Goh, T. W.; Xiao, C.; Maligal-Ganesh, R. V.; Li, X.; Huang, W. *Chem. Eng. Sci.* **2015**, *124*, 45−51.
(17) Matyjaszewski, K. *Macromolecules* **2012**, *45*, 4015−4039.

DOI: 10.1021/acscatal.6b02642
ACS Catal. 2017, 7, 338−342